2017 IEEE International Conference on Manipulation, Manufacturing and Measurement on the Nanoscale (3M-NANO)
7-11 August, Shanghai

The Effect of Loading Rate on the Measurement of Cellular Viscoelasticity Properties with Atomic Force Microscopy

Bo Wang [1], Wenxue Wang [*1], Yuechao Wang [1], Bin Liu [1] and Lianqing Liu [*1]
[1]State Key Laboratory of Robotics, Shenyang Institute of Automation, Chinese Academy of Sciences, Shenyang, 110016, China

Bo Wang [2]
[2]University of Chinese Academy of Sciences, Beijing 100049, China
*Corresponding author: wangwenxue@sia.cn; lqliu@sia.cn

***Abstract*—Organisms are composed by cells, and the cells can also reflect the physiology of creatures. The composition of a single cell and its cytoskeletal structure can be reflected by the mechanical properties of the cell. The cellular mechanical properties are correlated to the biological functions of the cell and its physiological activities. Therefore, establishing the mathematical model for the mechanical properties of single cells could provide the foundation for analyzing and regulating the physiological state of cells. In our previous work, we established a dynamical mathematical model with the viscose and elastic properties of single cells as the system parameters of the cellular system. The mathematical model can characterize the stress-relaxation phenomenon of a single cell, which is caused by an atomic force microscope (AFM). However, in this model, the effect of the loading rate of the AFM cantilever was neglected and all the stress-relaxation curves needed to be measured at a constant loading rate, in case that different loading rates would cause errors in the stress-relaxation curves. In this study, we discussed the effect of the loading rate on the measurement of cellular viscoelasticity properties with AFM. We clearly illustrated that the cellular stress-relaxation curves won't be effected by the loading rate of AFM when the loading rate is higher than a threshold. The stress-relaxation curves with the loading rate which is higher than the threshold can be used to extract viscoelasticity parameters more accurately.**

Keywords—single cell; dynamic model; mechanical properties; loading rate; viscoelasticity; atomic force microscope

I. INTRODUCTION

Organisms are composed by cells, and the cells can also reflect the physiology of creatures [1]. The composition of a single cell and its cytoskeletal structure can be reflected by the mechanical properties of the cell. The cellular mechanical properties are correlated to the biological functions of the cell and its physiological activities. Therefore, establishing the mathematical model for the mechanical properties of single cells could provide the foundation for analyzing and regulating the physiological state of cells. The mechanical properties of single cells are related to some diseases [2-4]. Recently, some nanotechnologies, such as the atomic force microscope (AFM), magnetic and optical tweezers [5], and micropipettes [6], offered approaches to measure the mechanical properties of single cells. Therefore, the mechanical information of single cells could be used as label-free biomarkers for the state evaluation of cells [7,8]. But a cell can be regarded as an extremely complex network, which include a large number of overlapping signaling pathways [9]. It is extremely difficult to depict the dynamical behavior by using a mathematical model [10].

Hertz model is a kind of common description of the contact problem of two elastic bodies with curved surfaces which is used in classical contact mechanics [11]. But the Hertz model has certain disadvantages which need to be handled. For example, the Hertz model presumes that materials in contact are a sphere and a flat plate, which are linearly elastic and isotropic. That in general does not holds for cells. On the other hand, the Hertz model can reflect only the elasticity of the cell. J. R. Dutcher et al. calculated the viscoelastic properties of cell envelope from the creep deformation curves of the cell [12]. They used a three-element standard solid model to describe the mechanical properties of the cells. A linear standard solid model was used by A. Yango et al. to determine the viscoelastic properties of soft materials [13]. They used the AFM to measure the creep response to a step signal in the stress-relaxation part of the experiment. We have previously demonstrated a generalized Maxwell model without a pre-assuming order for describing the mechanical viscoelastic properties, and the system order and parameters can be determined by using the system identification method from the input-output curves in the indentation process [14,15]. In this work, the order and coefficients of the generalized Maxwell model can be obtained by system identification approach. In this study, we determined the system order by the Hankel matrix method, and the coefficients can be calculated by least squares method. In our previous work [14,15], we used four different types of cells to verified the effectiveness of the mathematical model for the of cell stress-relaxation behaviors under a constant indentation depth. The four types of cells are MCF-7, HEK-293, L-929 and Neuro-2A cells. After analysis the experimental curves, we found that for all these four types of cells, the order of the mathematical model was calculated to be second, and for each system, five parameters could to be identified by the stress-relaxation curves. Then these five-parameter tuples can be used as biomarkers to classify different types of cells. However, in this model, the effect of the loading rate of AFM was neglected and all the stress-relaxation curves we measured were in a constant loading rate to avoid the error caused by different loading rates. In this study, we

discussed the effect of the loading rate on the measurement of cellular viscoelasticity properties with AFM. We demonstrated that the cellular stress-relaxation process won't be effected by the loading rate of AFM when the loading rate is higher than a threshold. The stress-relaxation curves with the loading rate which is higher than the threshold can be used to extract viscoelasticity parameters more accurately.

II. Materials and Methods

A. Preparation of Cells and Materials

In this study, the cell lines we used were acquired from the Institute Pasteur of Shanghai, Chinese Academy of Sciences (Shanghai). The three types of cells, MCF-7 cells, L-929 cells and HEK-293 cells, were cultured in Petri dishes and the concentration of each type of cells is about $1.3\times 10^6/cm^2$. Before we did experiments, the cells were cultured for 24 hours at 37°C in culture medium. The experiments were conducted at 25°C. Without loss of generality, we performed the indentation experiments with different batches of cells.

B. Indentation Process

A Bioscope Catalyst atomic force microscope (Bruker, USA) and an inverted microscope (Nikon, Japan) were used in this study. The model of the AFM probe that we used in the experiment was MLCT (Bruker, USA). The nominal coefficient of elasticity of the cantilever is 0.01 N/m. Thermal tune was used to calculate the actual value of the cantilever's coefficient, and the actual value of the cantilever's coefficient is about 0.08 N/m.

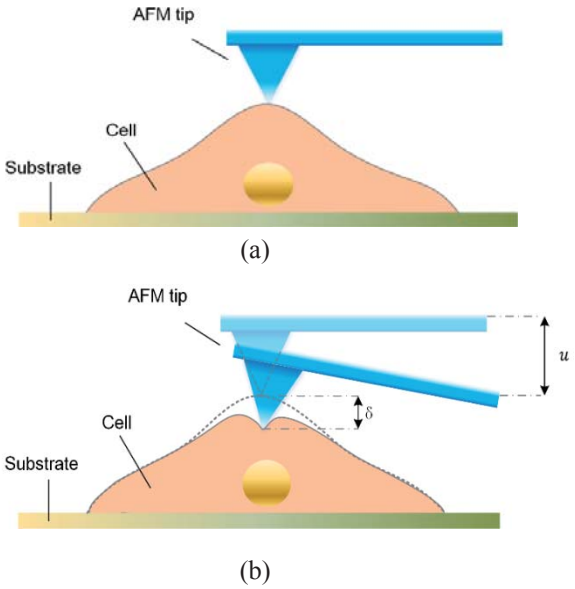

Fig. 1. Demonstration of a complete AFM indentation process. (a) Schematic diagram of the AFM tip contacting to the surface of a single cell. (b) Schematic diagram of the AFM tip pushing the cell and the cantilever deflecting correspondingly.

The standard AFM in dentation experiments were used to obtain the stress-relaxation curves of cells. In general, the indentation experiments can be divided into three different phases, that is, approaching, stress-relaxation, and retraction respectively. As shown is Fig. 1, in the approaching phase, the position of piezoelectric actuator (PZT) dropped with a constant speed and the cantilever deflected due to the contact with the cell. In the stress-relaxation phase, the PZT position was unchanging, and the cell continued deforming due to the stress-relaxation. In the retraction phase, the PZT position rose and the cell recovered from the deformation. The stress-relaxation time is 6 seconds, which can keep the stress-relaxation curves tend to steady. The maximal range of cantilever movement is 1 μm. In this indentation process, we used different loading rates to stimulate cells and measured the corresponding stress-relaxation curves. During both the first and last phase of the indentation process, the speed of PZT in the experiments of AFM indentation was kept constant.

C. Establishing the Mathematical Model of the Cellular Viscoelastic Properties

The state-space equations of the cellular system are as follows. A complete description of the modeling process can be found in [14,15].

$$\begin{cases} \dot{x}_i = -\frac{k_i}{b_i}x_i + \frac{k_i}{b_i}u\,, i = 1,2,\dots,n \\ y = -\sum_{i=1}^{n} k_i\, x_i + (k_0 + \sum_{i=1}^{n} k_i)u \end{cases} \quad (1)$$

where input of the system u and the output of the system y represent the PZT movement in z-position and interactive force between the AFM and the surface of the cell, respectively. The x_i is the state variable of the linear system and represents the movement of the virtual point between the spring element and damper element in the i^{th} pathway in the generalized Maxwell model. The corresponding elastic and viscous coefficients of the springs and dampers in the i^{th} pathway are k_i and b_i, respectively. It can be demonstrated by the dynamic model that the cellular viscoelasticity can be characterized by the coefficients k_i and b_i.

The order and coefficients of the generalized Maxwell model can be obtained by system identification approach. In this study, we determined the system order by the Hankel matrix method, and the coefficients can be calculated by least squares method. In our previous work [14,15], we used four different types of cells to verified the effectiveness of the mathematical model for the of cell stress-relaxation behaviors under a constant indentation depth. The four types of cells are MCF-7, HEK-293, L-929 and Neuro-2A cells. After analysis the experimental curves, we found that for all these four types of cells, the order of the mathematical model was calculated to be second. This denotes that the mechanical properties of single cells could be modeled as a second-order linear system, and for each system, five parameters could to be identified by the stress-relaxation curves.

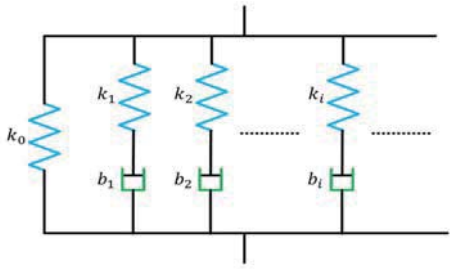

Fig. 2. Schematic of generalized Maxwell model which is composed by springs and dampers.

III. Results and Disscussion

Fig. 3 shows an entire indentation process, and in the stress-relaxation part, the force curve decreases from the peak and tend to converge to a constant. Under the assumption of generalized Maxwell model, we used MATLAB Simulink to simulate the different viscoelastic behaviors of cells under different loading rates. As is shown in Fig. 4 (a), the configuration of the simulation is a second-order Maxwell model, and Fig. 4 (b) shows the results of simulation under different loading rates

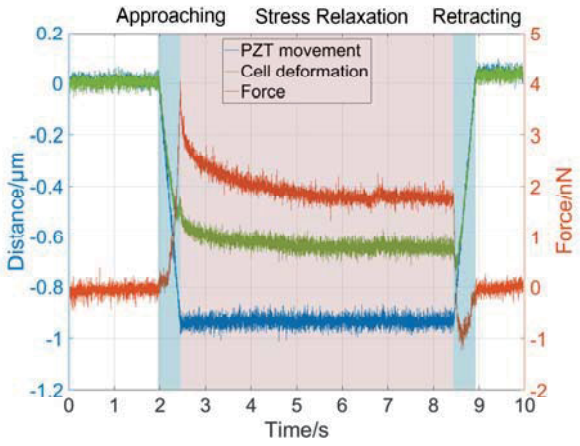

Fig. 3. A complete indentation process of a single cell, which was indented and measured by an AFM. The blue curve illustrates the different movement in the z-position of piezoelectric (PZT) during the three interaction phases. The red curve is the interaction force between the cell and the AFM tip which was measured by the AFM. The green curve was the cell deformation which was calculated by the mathematical model.

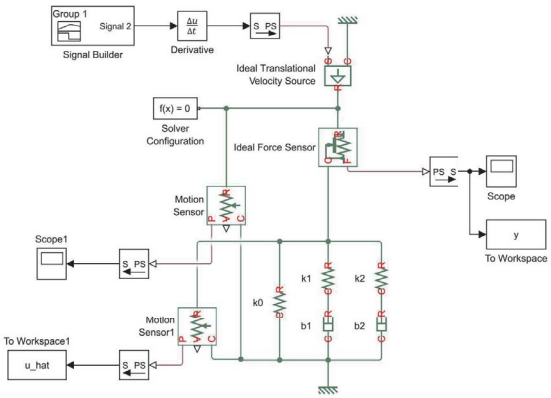

(a)

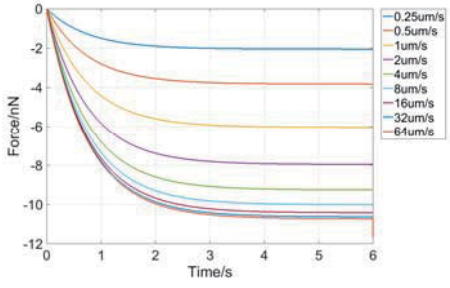

(b)

Fig. 4. A simulation of MATLAB Simulink. (a) The configuration of Simulink; (b) The results of simulation under different loading rates.

It can be seen from Fig. 4 (b) that as the loading rate increases, the stress-relaxation curves tend to be more precipitous and converge to the step response curve. Also, as the loading rate increases, the differences between two curves are tend to zero, which means that the stress relaxation curves are almost the same if the loading rate is higher. In fact, the force curves we measured contained noise and as the AFM loading rate increases and greater than a threshold, the stress-relaxation curves are coincident. As is shown in Fig. 5, the stress-relaxation curves tended to be the same as the loading rate increased, and when the loading rate is bigger than 8μm/s, the stress-relaxation curves overlap with each other, which means we could extract viscoelastic parameters without the effect of the loading rate. In order to verify the response pattern of different cells, the stress-relaxation curves of MCF-7 cells and HEK-293 cells were measured. The results showed that all these three types of cells have the same character that the stress-relaxation curves tend to be convergent as the loading rates increase, which means we can extract viscoelastic parameters without the effect of the loading rate.

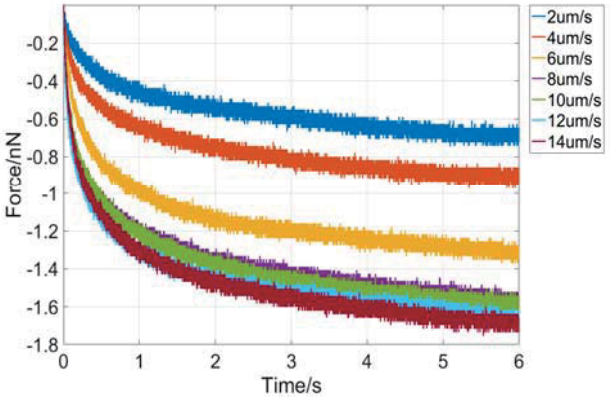

Fig. 5. The comparison of the stress-relaxation curves under different loading rates of a L-929 cell. The stress-relaxation curves tended to be the same as the loading rate increased.

We extracted viscoelastic parameters from stress-relaxation curves of L-929 cells under different loading rates, that is 2μm/s, 4μm/s, 6μm/s, 8μm/s, 10μm/s, 12μm/s and 14μm/s, as is shown in Table 1. Also, as the loading rates increased, the viscoelastic parameters tend to be convergent, because the effect of loading rate can be neglected when the AFM loading rate is high. Fig. 6 shows that the changes of viscoelastic parameters of L-929 cell under different loading rates. The first one is the change of the parameter k_0, the middle one and the last one are the changes of time constant $\frac{k_1}{b_1}$ and $\frac{k_2}{b_2}$. It can be seen from Fig. 6 that the trends of these three curves are firstly increasing, and then tend to be stable.

TABLE I. Viscoelastic Parameters of L-929 Cells Under Different Loading Rates

Loading Rates	k_0 (N/m)	k_1 (N/m)	b_1 (N·s/m)	k_2 (N/m)	b_2 (N·s/m)
2μm/s	0.3316	0.1398	0.0434	0.1906	0.8086
4μm/s	0.1659	0.2172	0.0430	0.3776	0.8322

Loading Rates	k_0 (N/m)	k_1 (N/m)	b_1 (N·s/m)	k_2 (N/m)	b_2 (N·s/m)
6μm/s	0.3821	0.2792	0.0556	0.2629	0.4757
8μm/s	0.3170	0.2991	0.0489	0.4045	0.8343
10μm/s	0.4041	0.3215	0.0517	0.3176	0.5830
12μm/s	0.3686	0.2795	0.0472	0.3694	0.7510
14μm/s	0.3669	0.3995	0.0594	0.3285	0.5956

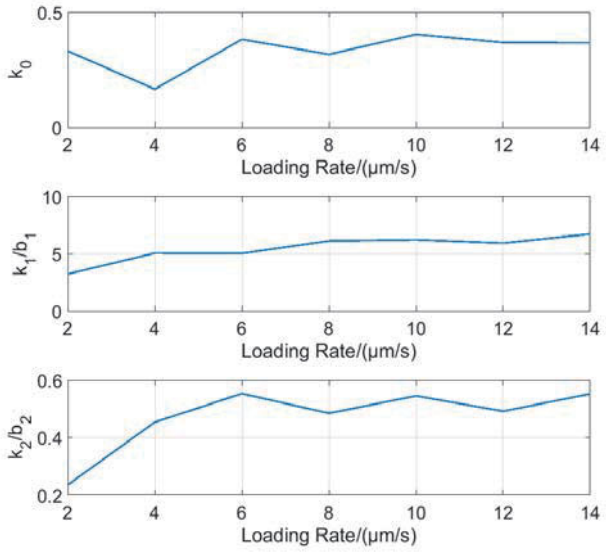

Fig. 6. Line charts of the viscoelastic parameters of L-929 cell under different loading rates. The first one is the change of the parameter k_0, the middle one and the last one are the changes of time constant $\frac{k_1}{b_1}$ and $\frac{k_2}{b_2}$.

IV. Conclusion

In this paper, the effect of the loading rate of AFM cantilever was considered in the model. In this study, we discussed the effect of the AFM loading rate of on the stress-relaxation curves, and we clearly illustrated that the cellular stress-relaxation curves won't be effected by the loading rate of AFM when the loading rate is higher than a threshold. The stress-relaxation curves with the loading rate which is higher than the threshold can be used to extract viscoelasticity parameters more accurately.

Acknowledgment

This work was supported by the National Natural Science Foundation of China (Grant Nos. 61433017, 61673372, 61327014 and 61522312) and the CAS/SAFEA International Partnership Program for Creative Research Teams.

References

[1] Zong, C.; Lu, S.; Chapman, A.R.; Xie, X.S. Genome-wide detection of single-nucleotide and copy-number variations of a single human cell. Science 2012, 338, 1622–1626.

[2] Plodinec, M.; Loparic, M.; Monnier, C.A.; Obermann, E.C.; Zanetti-Dallenbach, R.; Oertle, P.; Hyotyla, J.T.; Aebi, U.; Bentires-Alj, M.; Lim, R.Y.; et al. The nanomechanical signature of breast cancer. Nat. Nanotechnol. 2012, 7, 757–765.

[3] Yang, W.; Yu, H.; Li, G.; Wang, B.; Wang, Y.; Liu, L. Regulation of breast cancer cell behaviours by the physical microenvironment constructed via projection microstereolithography. Biomater. Sci. 2016, 4, 863–870.

[4] Yang, W.; Yu, H.; Li, G.; Wang, Y.; Liu, L. Facile modulation of cell adhesion to a poly (ethylene glycol) diacrylate film with incorporation of polystyrene nano-spheres. Biomed. Microdevices 2016, 18, 1–7.

[5] Li, X.; Yang, H.; Wang, J.; Sun, D. Design of a robust unified controller for cell manipulation with a robot-aided optical tweezers system. Automatica 2015, 55, 279–286.

[6] Guilak, F.; Tedrow, J.R.; Burgkart, R. Viscoelastic properties of the cell nucleus. Biochem. Biophys. Res. Commun. 2000, 269, 781–786.

[7] Shimizu, Y.; Kihara, T.; Haghparast, S.M.; Yuba, S.; Miyake, J. Simple display system of mechanical properties of cells and their dispersion. PLoS ONE 2012, 7, e34305.

[8] Lee, G.Y.; Lim, C.T. Biomechanics approaches to studying human diseases. Trends Biotechnol. 2007, 25, 111–118.

[9] Shimizu, Y.; Kihara, T.; Haghparast, S.M.; Yuba, S.; Miyake, J. Simple display system of mechanical properties of cells and their dispersion. PLoS One 2012, 7, e34305.

[10] Lee, G.Y.; Lim, C.T. Biomechanics approaches to studying human diseases. Trends Biotechnol 2007, 25, 111-118.

[11] Yang, W.; Yu, H.; Li, G.; Wang, B.; Wang, Y.; Liu, L. Regulation of breast cancer cell behaviours by the physical microenvironment constructed via projection microstereolithography. Biomater. Sci. 2016, 4, 863–870.

[12] Vadillo-Rodríguez, V.; Dutcher, J.R. Viscoelasticity of the bacterial cell envelope. Soft Matter 2011, 7, 4101.

[13] Yango, A.; Schape, J.; Rianna, C.; Doschke, H.; Radmacher, M. Measuring the viscoelastic creep of soft samples by step response afm. Soft Matter 2016, 12, 8297–8306.

[14] Wang B, Wang W, Wang Y, et al. Modeling and analysis of mechanical properties of single cells. Nano/Molecular Medicine and Engineering (NANOMED), The 10th IEEE International Conference on. IEEE, 2016.

[15] Wang, B.; Wang, W.; Wang, Y.; Liu, B.; Liu, L. Dynamical Modeling and Analysis of Viscoelastic Properties of Single Cells. Micromachines 2017, 8, 171.